Chemical Papers (2021) 75:205–214
https://doi.org/10.1007/s11696-020-01289-w

ORIGINAL PAPER

Microfluidics nanoprecipitation of telmisartan nanoparticles: effect of process and formulation parameters

Preena Shrimal[1] · Girirajsinh Jadeja[1] · Sanjaykumar Patel[1]

Received: 25 April 2020 / Accepted: 14 July 2020 / Published online: 19 July 2020

Abstract

A continuous microfluidic nanoprecipitation process has been investigated to prepare nanosized particles of a poorly water-soluble drug telmisartan (TEL), thereby enhancing its solubility and bioavailability. The present work aims to overcome agglomeration of drug particles by controlling the surface forces between the particles using various polymers like Polyvinylpyrrolidone K-30 (PVP K-30), Polyvinylpyrrolidone K-90 (PVP K-90), Poloxamer 188, Poloxamer 407, and hydroxypropyl methylcellulose (HPMC). The effect of process parameters such as solvent-to-antisolvent ratio, polymer-to-drug ratio, microchannel length, and solvent flow rate on drug particle size and polydispersity index (PDI) has been studied. The drug–polymer interaction investigated through X-ray diffraction (XRD) and Fourier transform infrared (FTIR) analysis revealed a significant reduction in peak intensity for Poloxamer 407 with no drug–polymer interaction. Also, the surface morphology of recrystallised TEL nanoparticles examined using field emission scanning electron microscopy (FESEM) showed clear and nearly uniform shaped particles. Poloxamer 407-based formulation of TEL exhibited minimum drug agglomeration with least particle size 369 nm and PDI value 0.049. The minimum particle size was achieved at solvent-to-antisolvent ratio 1:2, 1:1 polymer-to-drug ratio, microchannel length of 60 cm, and solvent flow rate of 30 mL/h. Thus, the microfluidic technique resulted in the production of TEL nanoparticles with narrow size distribution and useful morphological characteristics.

Graphic abstract

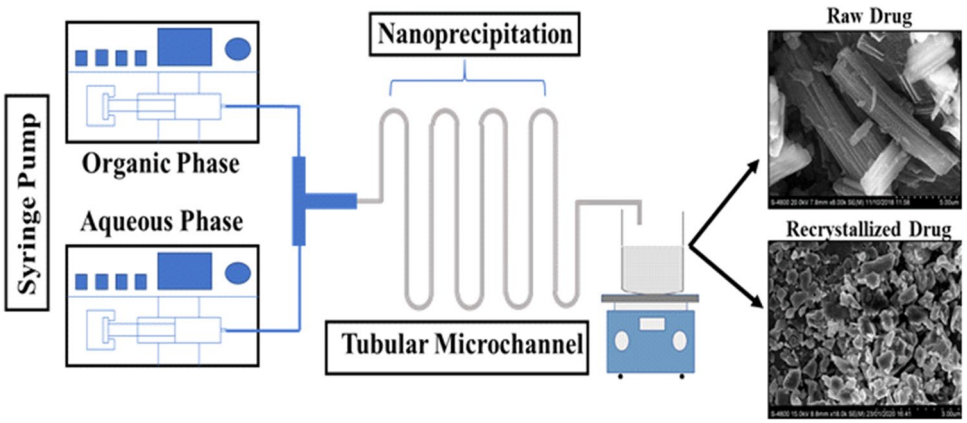

Keywords Microfluidics · Nanoprecipitation · Telmisartan · Solubility enhancement

Abbreviations

APIs	Active pharmaceutical ingredients
BCS	Biopharmaceutical Classification System
FESEM	Field emission scanning electron microscopy
FTIR	Fourier transform infrared
HPMC	Hydroxypropyl methylcellulose

✉ Sanjaykumar Patel
srpatel079@gmail.com

[1] Department of Chemical Engineering, S. V. National Institute of Technology, Surat, Gujarat 395007, India

PDI	Polydispersity index
PEO	Polyethylene oxide
PPO	Polypropylene oxide
PVP K-30	Polyvinylpyrrolidone K-30
PVP K-90	Polyvinylpyrrolidone K-90
TEL	Telmisartan
XRD	X-ray diffraction

Introduction

Over the last two decades, nanotechnology has gained great scientific interest with a significant impact in the field of chemistry, pharmaceutics, optics, electronics, and life sciences. The two most primitive methods for nanoparticles preparation are top-down and bottom-up approaches. In top-down approach, the particle size is reduced, employing mechanical forces. The major limitations involved with the top-down approach are long processing time, wider size distribution, and product contamination (Kakran et al. 2010); whereas, the bottom-up approach produces nanoparticles through a chemical reaction, nucleation, or self-assembly. The particles prepared by such a method suffer from uncontrolled particle growth which results in particle coagulation, aggregation, and agglomeration (Kaufman et al. 2012). Owing to these limitations, growth in microreactor technology in recent years has provided alternative process strategies.

Of late, microfluidics technology has shown its potential for continuous production of various nanosized particles by fluid diffusion, mixing, emulsification, or their combination (Feng et al. 2016). Benefiting from their inherent properties such as small channel dimensions, microreactor technology offers large surface-area-to-volume ratio, faster heat and mass transfer, and accordingly precise control of process parameters. Compared to the conventional batch approaches, microreactor technique provides a smaller particle size, smaller residence time, and narrow particle size distribution (Mello and Mello 2004). Microfluidic precipitation is an effective methodology to prepare nanoparticles and to encapsulate them. Here, the mixing time can be tuned quicker than that of time required for reagents to nucleate and grow. Subsequently, utilising this technology nanoprecipitation process, i.e. nucleation and crystal growth could be controlled separately as a component of microchannel length, thus avoiding particle agglomeration (Tai et al. 2016). Additionally, higher surface area-to-volume ratio and rapid heat and mass transfer results in monodispersed and reproducible nanoparticles (Shrimal et al. 2019b).

During the last two decades, nanoparticles have gained considerable interest in pharmaceutical industries. The major challenge for drug delivery scientists is preparation of active pharmaceutical ingredients (APIs) with enhanced solubility. The solubility of drug has a vital role in the field of drug delivery systems. At present, about 40% of the market formulations are poorly soluble in water (Khan et al. 2018). Solubility enhancement of poorly water-soluble APIs aids in achieving the required plasma concentration, thereby producing the desired pharmacological response. The conversion of drug particles into nanoparticles effectively enhances its aqueous solubility and bioavailability. TEL is one such drug which suffers from low aqueous solubility and poor bioavailability (Sharma et al. 2020). TEL, a well-known drug recommended to hypertension patients for prevention of strokes is a Biopharmaceutical Classification System (BCS) class-II drug. It is a selective angiotensin-II type-1 receptor, which acts by blocking the angiotensin receptor. The drug has high permeability and 0.09 mg/mL solubility in water with 42-58% low bioavailability (Sharma et al. 2018). It has the most prolonged half-life compared with any other angiotensin receptor. Hence, to improve TEL solubility, bioavailability, and to maximise the APIs efficacy drug nanonisation is a suitable approach according to Noyes Whitney equation (Hu et al. 2004).

Irrespective, of the approach utilised for preparing the nanoparticles, a major challenge in clinical translation of nanomedicine is their tendency to re-agglomerate. In antisolvent precipitation, as antisolvent is added to a solvent, rapid supersaturation is achieved resulting in production of nanosized particles. As the magnitude of inter-particulate van der Waal forces of attraction among formed nuclei increases, they tend to aggregate (Huang et al. 2008). To overcome this limitation, a stabiliser such as a polymer (steric stabilisation), a surfactant (electrostatic stabilisation), or a combination of both is used to retain the size of the nanoparticles. Polyvinylpyrrolidone (PVP) is an ionic, water-soluble polymer widely used in pharmaceutical industries for dispersing and suspending drugs. Offered in various range of molecular weight (2500–300000 g/mol) grades, they are characterised by K number. Poloxamers, also known by their trade name Pluronic®, are triblock copolymers consisting of polyethylene oxide (PEO) and polypropylene oxide (PPO) unit (PEO–PPO–PEO). Poloxamer, a non-ionic block copolymer is a white, coarse powder, and polymeric micelle carrier. Many researchers extensively use it as a solubiliser, stabiliser, and also as a surfactant. The solubility enhancement of drug using Poloxamer could be due to a reduction in surface tension and micellar solubilisation. Hydroxypropyl methylcellulose (HPMC) is a hydrophilic, biodegradable, and biocompatible polymer considered safe for human consumption. It is widely used in food and pharmaceutical industries as a stabiliser, emulsifier, and hydrophilic gel matrix material. Due to its excellent biocompatibility and low toxicity, it has gained the great interest of scientists and academicians for drug delivery applications.

In the present study, the solubility enhancement of TEL was attempted by drug particle size reduction using microfluidics nanoprecipitation technique. For this purpose, five different polymers (PVP K-30, PVP K-90, Poloxamer 188, Poloxamer 407, and HPMC) have been used to prepare TEL nanoparticles, and their impact on drug particle size and PDI were observed. By employing one factor at a time approach, the effect of various process and formulation parameters such as solvent-to-antisolvent ratio, polymer:drug ratio, microchannel length, and the solvent flow rate were investigated. FTIR analysis was performed to recognise the characteristic peak of pure TEL and recrystallised TEL. Moreover, pure drug and recrystallised drug using different polymers were analysed for XRD, and surface morphology was investigated using FESEM.

Materials and methods

Materials

Acetone and dichloromethane of analytical reagent grade were acquired from Finar Chemicals Ltd., Ahmedabad, India. Telmisartan was obtained from Ohm laboratory, Shilaj, Ahmedabad, India. The polymers used in this study were PVP K-30, PVP K-90 and HPMC purchased from Finar Chemicals, Ahmedabad, India. Poloxamer 407 & Poloxamer 188 were purchased from Sigma-Aldrich.

Methods

Nanoprecipitation of TEL

Continuous microchannel nanoprecipitation was used to prepare TEL nanoparticles. Five different polymers like PVP K-30, PVP K-90, HPMC, Poloxamer 407 and Poloxamer 188 were reported to be used were screened for selecting suitable polymer to prepare TEL nanoparticles. Each of them was dispersed in the aqueous phase (water). The organic phase was prepared dissolving 100 mg of telmisartan in 18 mL acetone and 2 mL dichloromethane. Two syringe pumps were used to deliver the solvent and antisolvent phase from Dispovan syringe to particular microchannel. The microfluidic device was fabricated in the lab using a 0.8-mm I.D. silicone tube. Silicone tube was mounted over a glass plate in a serpentine manner, as shown in Fig. 1. The serpentine shapes of the microchannel are used to accelerate mixing. Both the phases (solvents and antisolvent) were passed using silicon microchannel and at T-junction for the first time mixing of organic and aqueous phase begins because of micromixer geometry. Due to the inherent property of microreactor, the flow regimes in microchannels are generally laminar owing to diffusion-controlled mixing throughout (Patil et al. 2015). The turbulence created due to turns in microchannel ensures rapid nucleation and causes the breakdown of the particles, thereby preventing them from growing to a large size. From one end of silicon tube continuous product was obtained in a beaker, kept on stirring at 600 rpm for 45 min to evaporate the solvent. The resultant product was then centrifuged for 20 min at 15 °C and 17000 rpm. The pellet obtained after centrifuge was air-dried and stored for further analysis. The influence of various process and formulation parameters like a solvent-to-antisolvent ratio, polymer-to-drug ratio, microchannel length and solvent flow rate on nanoparticle size and PDI were evaluated. Solvent-to-antisolvent ratio was studied over 1:1.5 to 1:3 ratio; whereas, polymer-to-drug ratio was varied from 0.5 to 1.5. The effect of length of microchannel on particle size and PDI was investigated from 40 cm to 80 cm length. The solvent flow rate was varied between 20 and 50 mL/h.

Characterisation

Particle size and polydispersity index (PDI)

Particle size and PDI of prepared TEL nanosized particles were investigated using Zeta Sizer (Nano ZS90, Malvern Instruments Ltd., Worcestershire, U.K.) at 25 °C. The results reported in the present study for particle size are on the basis of volume distribution. Generally, the volume mean diameter

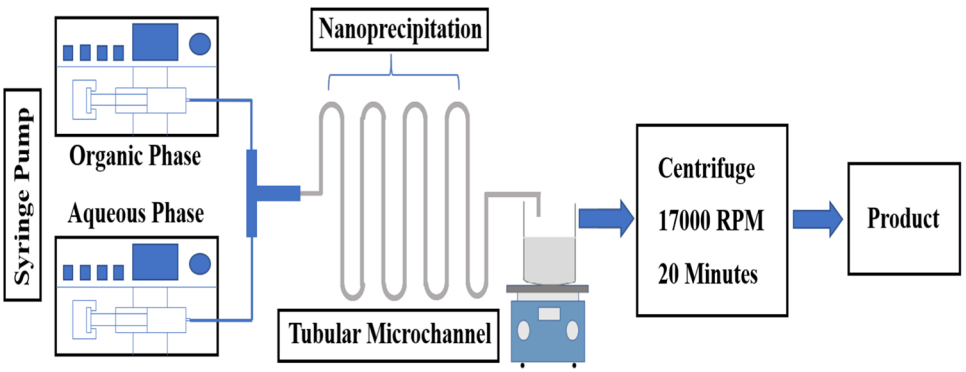

Fig. 1 Experimental setup for TEL nanoparticles preparation

is utilised to represent the stability of prepared particles (Malvern 2004).

Fourier transform infrared (FTIR) spectroscopy

The FTIR spectra of raw TEL and recrystallised TEL nanoparticles using PVP K-30, PVP K-90, HPMC, Poloxamer 407 and Poloxamer 188 were recognised through FTIR spectroscopy (FTIR-8400S with DRS, Shimadzu, Japan). For analysing the prepared formulation, 40 mg of KBr and 1 mg of prepared formulation was mixed to obtain the pellets. The spectra were recorded in the 4000–400 cm^{-1} wavelength range.

Field emission scanning electron microscopy (FESEM)

The surface morphology of recrystallised TEL formulation was characterised by FESEM (FESEM-S 4800, Hitachi, Japan). The operating conditions were 20 kV accelerating voltage and 15.2 mm working distance. Using double-sided tape, the prepared TEL particles were mounted over metal stub and gold-coated (Hitachi E1010) under vacuum.

X-ray diffraction (XRD) analysis

The raw and prepared TEL formulation obtained using PVP k-30, PVP K-90, HPMC, Poloxamer 407 and Poloxamer 188 were characterised using X-ray diffraction (XRD-6100, Shimadzu). The investigation utilised Cu Kα radiations with 40 kV monochromator voltage and 30 mA current. The continuous scan at 2 deg/min speed with step size 0.02° was performed in angle range $10° < 2\theta < 80°$.

Results and discussion

Effect of various polymers on drug particle size and PDI

As described in a classical nucleation theory by Ostwald–Miers, crystallisation begins as the degree of supersaturation becomes greater than the critical supersaturation ratio, nucleation occurs followed by crystal growth (Ozaki et al. 2012; Sangwal 2007). When the nuclei size formed is less than the critical size, the increment in interfacial energy is more than that of decrement in volume energy, and hence crystal does not grow further. Consequently, to retain a super-saturable state, an extra additive is required which controls the growth of formed nuclei. The presence of polymer/stabilisers, which undergo preferential adsorption at the particle surface further stops the growth of particles through steric or electrostatic stabilisation (Matteucci et al. 2006). Numerous hydrophilic and amphiphilic polymers, such as PVP, PEG, HPMC, Soluplus, and Poloxamers are recognised as effective excipients for nanoprecipitation (Li et al. 2010; Warren et al. 2010). In the present study, five different polymers were used to prepare TEL nanoparticles; these were HPMC, PVP K-30, PVP K-90, Poloxamer 407, and Poloxamer 188. The effect of these polymers over particle size and PDI of formed TEL nanoparticles was observed, as shown in Fig. 2.

The particles size of these batches ranged from 2302.6 nm to 1227.3 nm. Nanoparticles prepared using Poloxamer 188 reported the maximum particle size of 2302.6 nm with a PDI value of 0.36. The greatest particle size reduction was reported for Poloxamer 407, which might have shown greater adsorption potential at TEL surface. The driving force for Poloxamer 407 adsorption is the hydrophobic moiety of the copolymer. Lee et al. 2010 also reported that amphiphilic polymers such as Poloxamers are generally more efficient stabilisers for nanoparticles compared to hydrophilic polymers (HPMC, PVP) as they can decrease the interfacial tension and increase the wettability of nanocrystals (Lee et al. 2010). The value of particle size for five investigated polymers increases as follows: $d_{Poloxamer407} < d_{PVPK-30} < d_{HPMC} < d_{PVPK-90} < d_{Poloxamer188}$. Therefore, Poloxamer 407 showed the highest compatibility with TEL for particle stabilisation. The TEL particle size of 1227.3 nm and 0.316 PDI was reported for Poloxamer 407 keeping all other parameters constant. Bhise et al. 2011 also reported Poloxamer 407 as the best polymer among PVP K-30, HPMC E4, PEG 6000, and Gelucire 43/01 to enhance the dissolution rate of TEL (Bhise et al. 2011). Additionally, Khan et al. 2018 also reported Poloxamer 407 as a most suitable polymer among PVP K-30, HPMC 15 Cps, and Poloxamer 407 for preparing dexibuprofen nanocrystals using microchannel fluidic reactor (Khan et al. 2018).

X-ray diffraction patterns of pure TEL along with the formulation prepared using HPMC, PVP K-30, PVP K-90, Poloxamer 407, and Poloxamer 188 are shown in Fig. 3. The

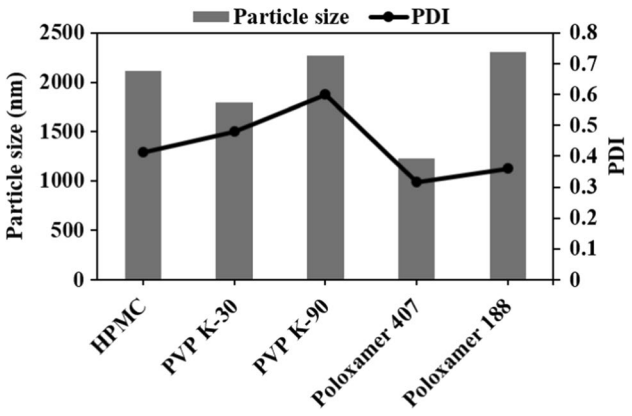

Fig. 2 Effect of various polymers on TEL particle size and PDI

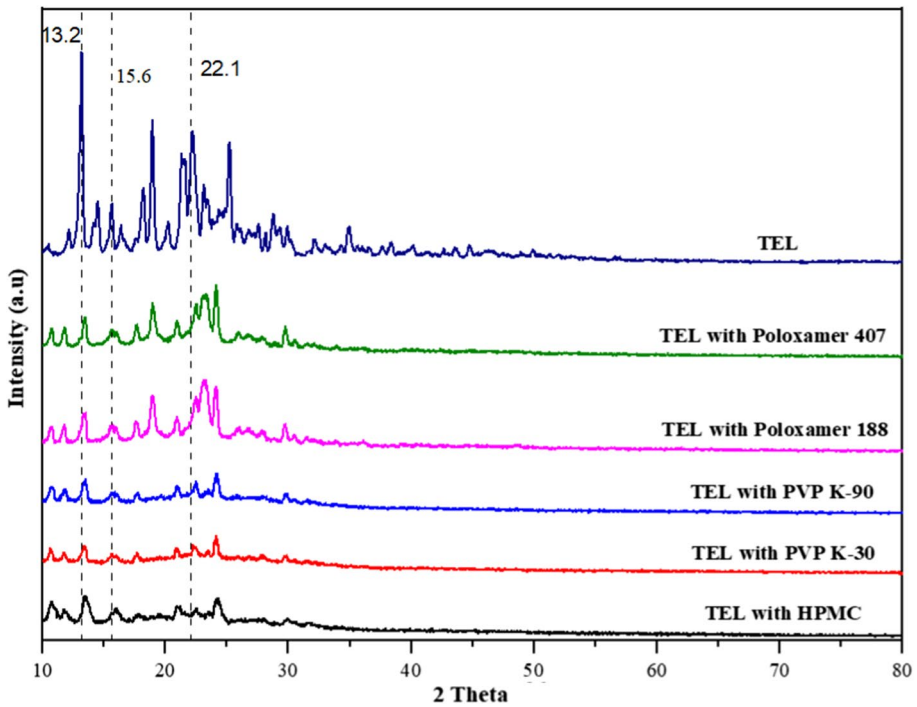

Fig. 3 XRD chromatogram of raw drug and recrystallised drug using different polymers

diffractogram of TEL showed characteristic intensity at a diffraction angle of 2θ at 13.2°, 14.5°, 15.6°, 18.2°, 21.6°, 22.1°, and 25.2° revealing that raw TEL present as crystalline form. The reduction in significant drug peak intensities was observed in all the formulations. It was noted that the major decrement in peak intensity was with PVP K-30. Moreover, Poloxamer 407 also showed nearly the same reduction in peak intensity. The trend observed for peak size reduction using different polymer was PVP K-30 < Poloxamer 407 < PVP K-90 < HPMC < Poloxamer 188. Thus, reduction in peak intensity of TEL, after processing by antisolvent precipitation supports the view that crystalline state has been shifted towards the amorphous solid state. This marked decrement in peak size explains the significant enhancement in the dissolution rate of TEL. Additionally, the same peak position of raw TEL and the nanosized TEL formulation proved that antisolvent precipitation of TEL nanoparticles did not alter the physical characteristics of the raw drug.

FTIR spectroscopy was performed as well to evaluate the molecular structure of TEL nanoparticles prepared using different polymers by microchannel precipitation technique. A possible interaction among TEL and polymer could result in change of functional group bonding which could be detected using FTIR spectroscopy. The drug molecule is dispersed inside the polymeric matrix, which enhances the interaction stability. The interaction between drug and polymer usually results in peak broadening and shifting of molecules functional groups (Frizon et al. 2013). Figure 4 shows the FTIR spectrum of raw TEL and recrystallised TEL using different polymers. The typical TEL spectra exhibit characteristic peaks at 1701 cm^{-1} assigned to the carboxyl group, and 1334 cm^{-1} for C–N stretch. In case of Poloxamer 407 all intrinsic absorption band of TEL was reported with no shift in wavenumber. It could be attributed to no interaction between TEL and Poloxamer 407; whereas, in the case of Poloxamer 188, the characteristic peak of carboxylic group at 1701 cm^{-1} was found absent. Also, for PVP K-30, PVP K-90, and HPMC, the presence and absence of characteristic peak related to TEL were observed. For PVP K-30, and PVP K-90 peak shifting or broadening was seen at 1701 cm^{-1} wavenumber. The shift observed in vibrational frequency corresponding to carboxylic acid suggests the TEL and polymer (Poloxamer 188, PVP K-30, PVP K-90, and HPMC) molecular interaction (Chae et al. 2018; Sharma et al. 2019). Moreover, for HPMC, both the characteristic peaks of TEL were absent. Hence, it could be summarised that no interaction between TEL and polymer was observed in case of recrystallisation with Poloxamer 407; whereas, for Poloxamer 188, PVP K-30, PVP K-90, and HPMC recrystallised drug interact with polymers (Sangwai and Vavia 2013).

Effect of solvent-to-antisolvent ratio on drug particle size and PDI

The impact of the solvent-to-antisolvent ratio on TEL crystal size and PDI was examined over four different ratios, i.e. 1:1.5, 1:2, 1:2.5, and 1:3, at drug-to-polymer ratio 1:1, with tube length 70 cm, and solvent flow rate 20 mL/h. No large variation in crystal size was observed while changing the

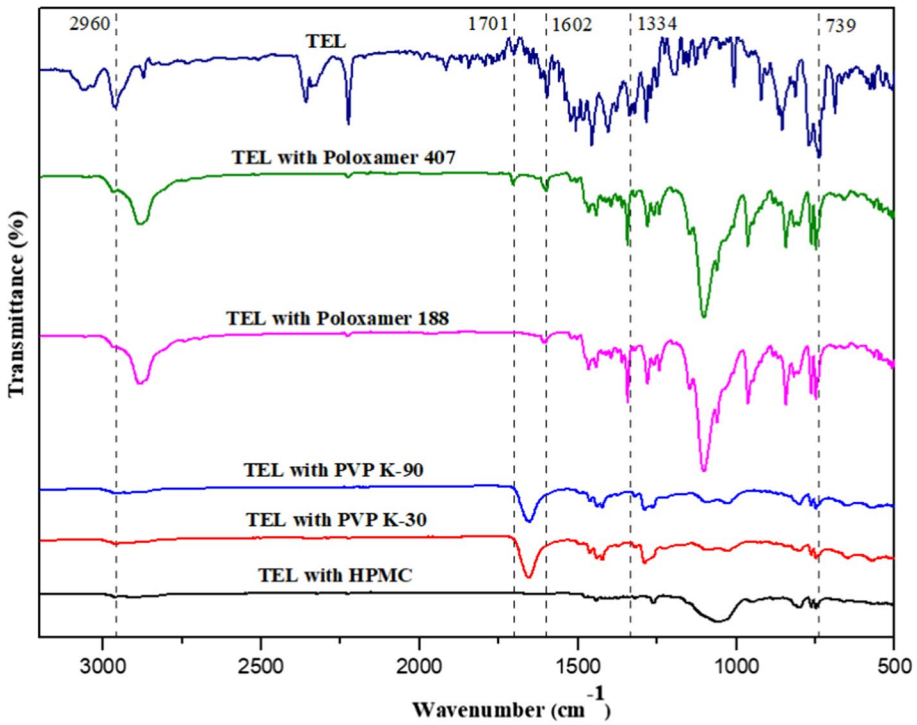

Fig. 4 FTIR spectra of raw drug and recrystallised drug using different polymers

solvent-to-antisolvent ratio. As the amount of antisolvent was increased from 1:1.5 to 1:2, the nanoparticle size was decreased from 602.7 to 508.4 nm with PDI variation from 0.355 to 0.236. It could be due to a large amount of aqueous phase volume resulting in higher nucleation rate and generation of smaller nuclei, and simultaneously particles grow. In the growth section, with increase in antisolvent volume diffusion distance increase, and consequently diffusion becomes a limiting step for growing crystal (Kakran et al. 2012). In comparison with crystal growth supersaturation greatly affects the nucleation rate. Therefore, high supersaturation results in more nuclei production and ultimately smaller size particles (Wang et al. 2007). Moreover, the increased antisolvent amount lowers the particle colliding frequency which reduces the particle aggregation possibility, which could also be justified by the low value of PDI. The smaller crystal size at a high solvent-to-antisolvent ratio was also obtained by Othman et al. 2015 in the production of polymeric nanoparticles through nanoprecipitation using flow focusing glass capillary microfluidic device for pharmaceutical application (Othman et al. 2015). However, further, increase in organic-to-aqueous phase volume ratio from 1:2 to 1:2.5 and 1:3 crystals with increased particle size was observed. This situation can be ascribed to the fact that the viscous forces become less significant as the volume of aqueous phase increases. The increase in PDI value from 0.236 to 0.429 also reveals the particle aggregation at higher antisolvent volume as shown in Fig. 5. Similarly, de Solorzano et al. 2016 also reported that increasing

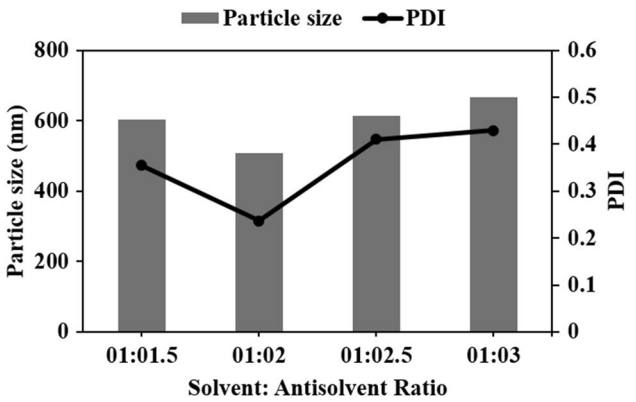

Fig. 5 Effect of solvent-to-antisolvent ratio on TEL particle size and PDI

aqueous-to-organic phase ratio there was an increase in particle size of cyclosporin-loaded PLGA nanoparticles by using interdigital microfluidic reactor. The best results were obtained when antisolvent-to-solvent ratio was 2 (de Solorzano et al. 2016).

Effect of polymer-to-drug ratio on drug particle size and PDI

The ratio of polymer:drug is an important factor in the present investigation. The polymer-to-drug ratio was investigated between 0.5 and 1.5 by keeping constant solvent flow rate 20 mL/h, microchannel length 70 cm,

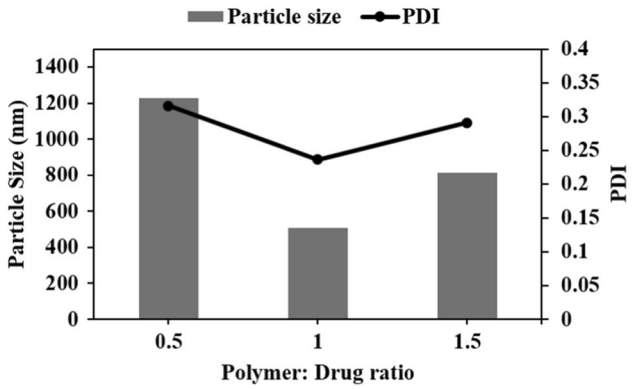

Fig. 6 Effect of polymer-to-drug ratio on TEL particle size and PDI

solvent-to-antisolvent ratio 1:2. The influence of polymer-to-drug ratio on TEL nanoparticle size and PDI was observed and summarised in Fig. 6. From the figure, it was observed that an increment in polymer concentration leads to a decrement in nanoparticle size from 1227.3 to 508.4 nm. This could be due to the ability of Poloxamer 407 to reduce the interfacial tension and hence the interfacial free energy, which reduces the nanoparticle size and enhances the stability. The decrement in PDI value from 0.316 to 0.236 supports the improvement in nanoparticle stability. As it can be noticed, the smallest crystal size was obtained with a formulation having drug-to-polymer ratio 1:1. It might be due to the fact that at same molar ratio of TEL and Poloxamer 407, the amount of polymer was sufficient to retain the particle stability (Dora et al. 2010). Further increasing the polymer concentration, larger nanoparticles were formed. Such behaviour can be understood as more polymers could be absorbed into each nanoparticle so that its volume might be increased. Principally, at higher concentration, non-uniform supersaturation occurs, which results in bigger size nanoparticles through agglomeration or crystal growth (Zhang et al. 2010). The increase in polymer concentration increases the viscosity of the aqueous phase, which exerts the stabilising effect of Poloxamer 407. Enough high viscosity results in smaller crystal size and narrow particle size distribution. But, as the concentration of polymer was increased hydrophilic part of one crystal may interact with a hydrophilic part of another crystal, and this interparticle interaction of chain might create the particle agglomeration at higher concentration. Moreover, at greater concentration, the growth of formed nanoparticles occurs through condensation and coagulation phenomenon; hence larger size crystals are formed.

Effect of microchannel length on drug particle size and PDI

In this set of experiments, the microchannel length varied from 40 to 80 cm to study its effect on TEL particle size and PDI, while keeping other parameters constant (1:2 solvent-to-antisolvent ratio, polymer-to-drug ratio of 1:1, and solvent flow rate at 20 mL/h). As the microchannel length increases, TEL crystal size decreased to 423.65 nm at 60 cm length as compared to 729.6 nm at 40 cm microchannel length. Also, the PDI value decreased from 0.65 to 0.115 while increasing the microchannel length. Thus, microchannel length has a vital role in decreasing the drug particles size as well as for producing the nanosuspension with reduced tendency of particle agglomeration. This phenomenon could be due to the presence of many free drug particles in outlet suspension while the microchannel length was comparatively short due to inadequate mixing time, which leads to larger size crystals. Furthermore, at less residence time nanoparticles agglomerates, and many drug particles cannot diffuse together (Zhang et al. 2018). In case of larger microchannel length than 60 cm, the particle size of TEL crystals was found to be increasing from 423.65 to 935 nm. The PDI value also showed the same trend of increment from 0.115 to 0.85. According to Wu et al. 2017 at a higher length of the microchannel, the increase in drug crystal size could be due to the growth of particles through Ostwald ripening (Wu et al. 2017). Moreover, at greater tube length bigger size particles are produced since free TEL nanoparticles are almost incorporated. The results of the relationship between the particle size and PDI value with microchannel length are shown in Fig. 7.

Effect of solvent flow rate on drug particle size and PDI

The fluid flow in the microfluidic device is a diffusion-based laminar flow due to low Reynolds number (generally less than 500). Within the microchannel, mixing of the aqueous phase and organic phase occurs only through diffusion, and the solvent flow rate is considered as a critical parameter to control drug nanoprecipitation process.

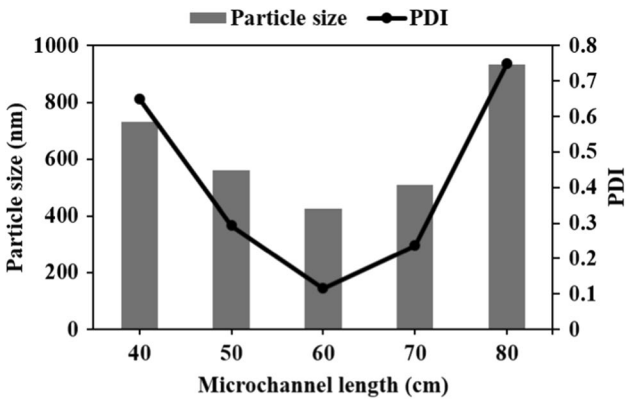

Fig. 7 Effect of microchannel length on TEL particle size and PDI

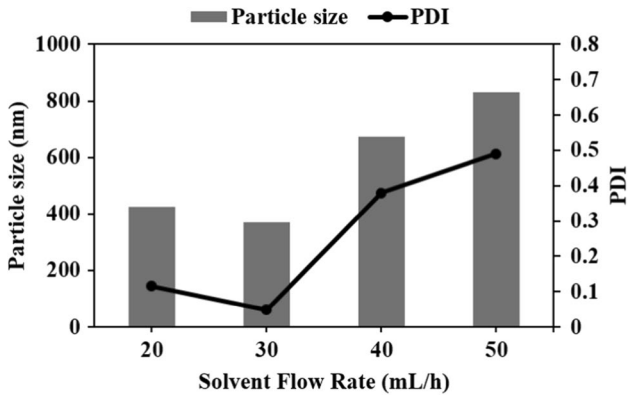

Fig. 8 Effect of solvent flow rate on TEL particle size and PDI

Moreover, this parameter directly influences nanoparticles features greatly. The influence of solvent flow rate on the resulting drug crystal size and PDI of TEL nanoparticles were investigated at 20, 30, 40, and 50 mL/h (Fig. 8). In this study, the solvent-to-antisolvent ratio of 1:2, polymer-to-drug ratio 1:1, microchannel length of 60 cm were kept constant. It has been observed that on increasing solvent flow rate from 20 to 30 mL/h, the particle size and PDI of formed TEL nanoparticles decreased significantly. This might be because of increase in flow rate increases the jet velocity, the Reynolds number, and shear forces thus increasing to the extent of mixing between organic phase and aqueous phase per unit time (Kakran et al. 2012). Zhang et al. 2018 also reported that at high Reynolds number, better mixing performance consumes more free drug particles to generate crystal nuclei individually, contributing to smaller size nanoparticles (Zhang et al. 2018). A fast flow results in rapid convective mixing, avoiding the formation of bigger size crystals (de Solorzano et al. 2016). As solvent flow rate increases, the crystal size was decreased to 369.9 nm with PDI of 0.049. Further, it was noted that with at a fast solvent flow rate, large size nanocrystals were formed. As the increased solvent flow rate caused inadequate blending of solvent and antisolvent in the mixing channel due to which solvent diffusion and the transfer was not completed, and it could generate non-uniform region supersaturation, subsequently forming larger size crystals. This effect dominated over the positive contribution of the increase of Reynolds number and hence resulted in increased crystal size (Wang et al. 2010). Moreover, increased flow rate results in enhanced mixing, which will improve particle concentration and increase the probability of particle aggregation (Dong et al. 2019). The increase in PDI value also reports the broad particle size distribution as the flow rate increased from 30 mL/h to 40 and 50 mL/h.

Particle size distribution and polydispersity index

Figure 9 shows the particle size distribution statistic by volume graph for TEL nanoparticles using Poloxamer 407 at a solvent-to-antisolvent ratio of 1:2, polymer-to-drug ratio 1:1, microchannel length 60 cm, and solvent flow rate 30 mL/h. The average TEL nanoparticle size at these conditions was observed to be 369 nm with a PDI value 0.04. The PDI value smaller than 0.2 indicates the narrow particle size distribution of the crystals under investigation (Landry et al. 2008). Thus, the decrement in TEL particle size would result in TEL solubility enhancement and bioavailability improvement (Shrimal et al. 2019a).

Field emission scanning electron microscopy (FESEM)

Figure 10a exhibits the surface morphology of raw TEL particles and Fig. 10b shows the FESEM image of the recrystallised TEL nanoparticles prepared through microfluidics at a solvent-to-antisolvent ratio of 1:1, polymer-to-drug ratio 1:1, microchannel length 60 cm, and solvent flow rate of 30 mL/h. It was observed that raw TEL showed rod-shaped, large, and irregular surface characteristics. The average particle size of raw TEL particles was about 10 µm. Moreover, the prepared TEL formulation showed a marked reduction in drug particle size and altered the morphology of TEL in a clear and nearly uniform shape. The drastic changes in shape and appearance in the particles suggest the effectiveness of microchannel nanoprecipitation technique.

Conclusion

Here, in the study microfluidic nanoprecipitation technique was found to be a promising technology for drug crystal size reduction to nano-range. The most suitable polymer was

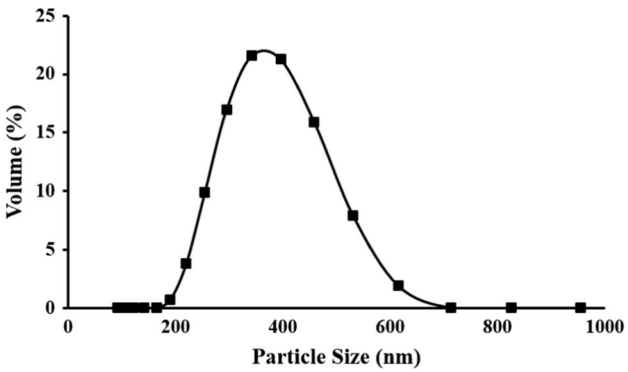

Fig. 9 Particle size distribution statistic graph for prepared TEL nanoparticles at optimum condition

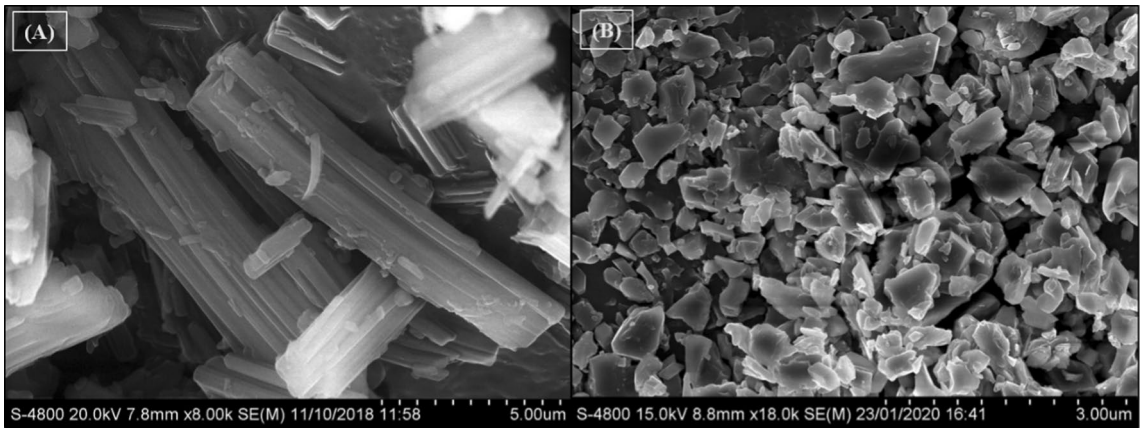

Fig. 10 FESEM images of **a** raw drug **b** recrystallised drug using microfluidics at optimum conditions

found to be Poloxamer 407 with respect to minimum particle size and particle aggregation. The minimum particle size of 369 nm with PDI value 0.049 was obtained for solvent-to-antisolvent ratio 1:2, polymer-to-drug ratio 1:1, microchannel length 60 cm, and solvent flow rate 30 mL/h. The recrystallized TEL nanoparticles showed clear and nearly uniform shape surface morphology.

Acknowledgements The corresponding author would like to acknowledge Science and Engineering Research Board, Department of Science and Technology, Government of India (sanctioned no. EEQ/2018/001001, dated 23-05-2019) for financial support.

Compliance with ethical standards

Conflict of interest On behalf of all authors, the corresponding author reports there is no conflict of interest.

References

Bhise S, Mathure D, Patil MV, Patankar RD (2011) Solubility enhancement of antihypertensive agent by solid dispersion technique. Int J Pharm Life Sci 2:970–995

Chae JS et al (2018) Tablet formulation of a polymeric solid dispersion containing amorphous alkalinized telmisartan. AAPS PharmSciTech 19:2990–2999

de Solorzano IO, Uson L, Larrea A, Miana M, Sebastian V, Arruebo M (2016) Continuous synthesis of drug-loaded nanoparticles using microchannel emulsification and numerical modeling: effect of passive mixing. Int J Nanomed 11:3397

Dong Z, Rivas DF, Kuhn S (2019) Acoustophoretic focusing effects on particle synthesis and clogging in microreactors. Lab Chip 19:316–327

Dora CP, Singh SK, Kumar S, Datusalia AK, Deep A (2010) Development and characterization of nanoparticles of glibenclamide by solvent displacement method. Acta Pol Pharm 67:283–290

Feng Q, Sun J, Jiang X (2016) Microfluidics-mediated assembly of functional nanoparticles for cancer-related pharmaceutical applications. Nanoscale 8:12430–12443

Frizon F, de Oliveira Eloy J, Donaduzzi CM, Mitsui ML, Marchetti JM (2013) Dissolution rate enhancement of loratadine in polyvinylpyrrolidone K-30 solid dispersions by solvent methods. Powder Technol 235:532–539

Hu J, Johnston KP, Williams RO III (2004) Nanoparticle engineering processes for enhancing the dissolution rates of poorly water soluble drugs. Drug Dev Ind Pharm 30:233–245

Huang Q-P, Wang J-X, Chen G-Z, Shen Z-G, Chen J-F, Yun J (2008) Micronization of gemfibrozil by reactive precipitation process. Int J Pharm 360:58–64

Kakran M, Sahoo N, Li L, Judeh Z, Wang Y, Chong K, Loh L (2010) Fabrication of drug nanoparticles by evaporative precipitation of nanosuspension. Int J Pharm 383:285–292

Kakran M, Sahoo NG, Tan I-L, Li L (2012) Preparation of nanoparticles of poorly water-soluble antioxidant curcumin by antisolvent precipitation methods. J Nanoparticle Res 14:757

Kaufman JJ et al (2012) Structured spheres generated by an in-fibre fluid instability. Nature 487:463–467

Khan J, Bashir S, Khan MA, Mohammad MA, Isreb M (2018) Fabrication and characterization of dexibuprofen nanocrystals using microchannel fluidic rector. Drug Des Devel Ther 12:2617

Landry V, Riedl B, Blanchet P (2008) Alumina and zirconia acrylate nanocomposites coatings for wood flooring: photocalorimetric characterization. Prog Org Coat 61:76–82

Lee M, Kim S, Ahn C-H, Lee J (2010) Hydrophilic and hydrophobic amino acid copolymers for nano-comminution of poorly soluble drugs. Int J Pharm 384:173–180

Li DX et al (2010) Enhanced oral bioavailability of flurbiprofen by combined use of micelle solution and inclusion compound. Arch Pharmacal Res 33:95–101

Malvern I (2004) Zetasizer nano series user manual. Malvern Instruments Ltd, Worcestershire

Matteucci ME, Hotze MA, Johnston KP, Williams RO (2006) Drug nanoparticles by antisolvent precipitation: mixing energy versus surfactant stabilization. Langmuir 22:8951–8959

Mello Jd, Mello Ad (2004) FocusMicroscale reactors: nanoscale products. Lab Chip 4:11N–15N

Othman R, Vladisavljević GT, Nagy ZK (2015) Preparation of biodegradable polymeric nanoparticles for pharmaceutical applications using glass capillary microfluidics. Chem Eng Sci 137:119–130

Ozaki S, Minamisono T, Yamashita T, Kato T, Kushida I (2012) Supersaturation–nucleation behavior of poorly soluble drugs and its impact on the oral absorption of drugs in thermodynamically high-energy forms. J Pharm Sci 101:214–222

Patil P, Khairnar G, Naik J (2015) Preparation and statistical optimization of Losartan Potassium loaded nanoparticles using Box Behnken factorial design: Microreactor precipitation. Chem Eng Res Des 104:98–109

Sangwai M, Vavia P (2013) Amorphous ternary cyclodextrin nanocomposites of telmisartan for oral drug delivery: improved solubility and reduced pharmacokinetic variability. Int J Pharm 453:423–432

Sangwal K (2007) Additives and crystallization processes: from fundamentals to applications. John Wiley & Sons, Chichester

Sharma C, Desai MA, Patel SR (2018) Ultrasound-assisted anti-solvent crystallization of telmisartan using dimethyl sulfoxide as organic solvent. Cryst Res Technol 53:1800001

Sharma C, Desai MA, Patel SR (2019) Effect of surfactants and polymers on morphology and particle size of telmisartan in ultrasound-assisted anti-solvent crystallization. Chem Pap 73:1685–1694

Sharma C, Desai MA, Patel SR (2020) Anti-solvent sonocrystallization for nano-range particle size of telmisartan through Taguchi and Box-Behnken design. Chem Pap 74:323–331

Shrimal P, Jadeja G, Naik J, Patel S (2019a) Continuous microchannel precipitation to enhance the solubility of telmisartan with poloxamer 407 using Box-Behnken design approach. J Drug Deliv Sci Technol 53:101225

Shrimal P, Jadeja G, Patel S (2019b) A review on novel methodologies for drug nanoparticle preparation: microfluidic approach. Chem Eng Res Des

Tai S, Zhang W, Zhang J, Luo G, Jia Y, Deng M, Ling Y (2016) Facile preparation of UiO-66 nanoparticles with tunable sizes in a continuous flow microreactor and its application in drug delivery. Microporous Mesoporous Mater 220:148–154

Wang Z, Chen JF, Le Y, Shen ZG, Yun J (2007) Preparation of ultrafine beclomethasone dipropionate drug powder by antisolvent precipitation. Ind Eng Chem Res 46:4839–4845

Wang JX, Zhang QX, Zhou Y, Shao L, Chen JF (2010) Microfluidic synthesis of amorphous cefuroxime axetil nanoparticles with size-dependent and enhanced dissolution rate. Chem Eng J 162:844–851

Warren DB, Benameur H, Porter CJ, Pouton CW (2010) Using polymeric precipitation inhibitors to improve the absorption of poorly water-soluble drugs: a mechanistic basis for utility. J Drug Target 18:704–731

Wu K-J, Bohan GMDV, Torrente-Murciano L (2017) Synthesis of narrow sized silver nanoparticles in the absence of capping ligands in helical microreactors. React Chem Eng 2:116–128

Zhang H-X, Wang J-X, Shao L, Chen J-F (2010) Microfluidic fabrication of monodispersed pharmaceutical colloidal spheres of atorvastatin calcium with tunable sizes. Ind Eng Chem Res 49:4156–4161

Zhang X, Chen H, Qian F, Cheng Y (2018) Preparation of itraconazole nanoparticles by anti-solvent precipitation method using a cascaded microfluidic device and an ultrasonic spray drier. Chem Eng J 334:2264–2272